Hydrogen Storage

DOI: 10.1002/ange.200801488

A Comparison of the H_2 Sorption Capacities of Isostructural Metal–Organic Frameworks With and Without Accessible Metal Sites: $[\{Zn_2(abtc)(dmf)_2\}_3]$ and $[\{Cu_2(abtc)(dmf)_2\}_3]$ versus $[\{Cu_2(abtc)\}_3]$**

*Yong-Gon Lee, Hoi Ri Moon, Young Eun Cheon, and Myunghyun Paik Suh**

Various metal–organic frameworks (MOFs) have been prepared to obtain materials that show specific or multifunctional properties. Porous MOFs that contain free space where guest molecules can be accommodated are of particular interest because they can be applied in gas storage[1–4] and separation,[4–6] selective adsorption and separation of organic molecules,[1,7] ion exchange,[8] catalysis,[9] sensor technology,[1,10] and for the fabrication of metal nanoparticles.[11] Secondary building units (SBUs) with a specific geometry have often been employed[12] for the modular construction of porous MOFs as they make the design and prediction of molecular architectures simple and easy. In particular, $\{M_2(CO_2)_4\}$-type paddlewheel clusters that can be formed from the solvothermal reaction of M^{2+} ions and the appropriate carboxylic acid are widely used for the construction of porous frameworks. Three-dimensional porous frameworks with various topologies (Pt_3O_4, boracites, NbO, and PtS nets) can be built from paddlewheel-type metal cluster SBUs and tri- or tetracarboxylates,[13–16] whereas pillared square-grid networks can be constructed from paddlewheel cluster SBUs and dicarboxylates in the presence of diamine ligands.[17]

Porous MOFs with accessible metal sites (AMSs) should have a higher hydrogen storage capacity than those without AMSs,[14,18] although there are not yet enough experimental data to support this assumption. To determine the effect of AMSs in a MOF on H_2 adsorption, the H_2 uptakes should be compared for the same framework in the absence and presence of AMSs, or for two independent isostructural MOFs with and without AMSs. H_2 uptake has previously been measured under several different outgassing conditions.[13] Unfortunately, these experiments could not clearly demonstrate the effect of AMSs as the exact formula and structure at each stage were not known. Furthermore, even when coordinating solvent molecules are successfully removed with retention of the porous framework structure, the metal ion sometimes transforms its coordination geometry to the thermodynamically most stable form instead of keeping the AMSs.[4,19]

Herein we report two porous MOFs with the same NbO-type net topology, namely $[\{Zn_2(abtc)(dmf)_2\}_3]\cdot 4H_2O\cdot 10dmf$ (**1**) and $[\{Cu_2(abtc)(H_2O)_2\}_3]\cdot 10dmf\cdot 6(1,4\text{-dioxane})$ (**2**; H_4abtc = 1,1′-azobenzene-3,3′,5,5′-tetracarboxylic acid[20]), and compare the gas adsorption data for the MOFs with and without AMSs.[21] Heating crystals of **1** and **2** under precisely controlled conditions allowed us to prepare $[\{Zn_2(abtc)(dmf)_2\}_3]$ (**1a**; SNU-4) and $[\{Cu_2(abtc)(dmf)_2\}_3]$ (**2a**; SNU-5′), which have no AMSs, as well as $[\{Cu_2(abtc)\}_3]$ (**2b**; SNU-5), which has AMSs. The framework structure of **1a** is the same as that of **1** and those of **2a** and **2b** are the same as that of **2**, as evidenced by the PXRD patterns. Solid **1a**, **2a**, and **2b** exhibit higher adsorption capabilities for N_2, CO_2, CH_4, and H_2 than other previously reported MOFs. In particular, **2b** adsorbs 2.87 wt% of H_2 gas at 77 K and 1 atm, which is the highest value for H_2 sorption under these conditions amongst a variety of other MOFs. The N_2, CO_2, and CH_4 adsorption capacities per unit sample volume for **2b**, which has AMSs, are 140–160% higher than those for **1a** and **2a**, which have no AMSs. The H_2 adsorption capacity of **2b** is also higher than those of **1a** and **2a** [at 77 K and 1 atm, 2.87 wt% for **2b** vs. 2.07 wt% for **1a** and 1.83 wt% for **2a**; excess adsorbed H_2 at 77 K and 50 bar: 5.22 wt% (total 6.76 wt%) for **2b** vs. 3.70 wt% (total 4.49 wt%) for **1a**], although this is mainly due to the lower molecular weight effect of **2b**. The H_2 sorption capacity ratios **2b**/**1a** and **2b**/**2a** per unit sample volume at 77 K and 1 atm are 105% and 120%, respectively, and the ratio **2b**/**1a** at 77 K and 50 bar is 106%. Our measurements of the isosteric heat of H_2 adsorption (zero-coverage isosteric heats are 7.24, 6.53, and 11.60 kJmol^{-1} for **1a**, **2a**, and **2b**, respectively) suggest that the enhanced H_2 adsorption in **2b** can be attributed to the stronger interaction of H_2 molecules with the AMSs of the MOF.

Yellowish block-shaped crystals of $[\{Zn_2(abtc)(dmf)_2\}_3]\cdot 4H_2O\cdot 10dmf$ (**1**) were prepared by heating a dmf solution of $Zn(NO_3)_2\cdot 6H_2O$ and H_4abtc at 100 °C for 12 h. Greenish block-shaped crystals of $[\{Cu_2(abtc)(H_2O)_2\}_3]\cdot 10dmf\cdot 6(1,4\text{-dioxane})$ (**2**) were prepared by heating $Cu(NO_3)_2\cdot xH_2O$ and H_4abtc in a dmf/1,4-dioxane/H_2O (4:3:1 v/v) mixture at 80 °C for 24 h. Solid **1** is insoluble in common organic solvents but is slightly soluble in water, where it dissociates into its building blocks. Solid **2** is insoluble in all common organic solvents and water. The temperature-dependent PXRD patterns show that the framework struc-

[*] Y.-G. Lee, H. R. Moon, Y. E. Cheon, Prof. M. P. Suh
Department of Chemistry, Seoul National University
Seoul 151-747 (Republic of Korea)
Fax: (+82) 2-886-8516
E-mail: mpsuh@snu.ac.kr

[**] This work was supported by a Korea Research Foundation Grant funded by the Korean Government (MOEHRD, Basic Research Promotion Fund; grant no. KRF-2005-084-0C00020) and by the Korea Science and Engineering Foundation (grant KOSEF, R11-2005-008-00000-0), Republic of Korea. H_4abtc = 1,1′-azobenzene-3,3′,5,5′-tetracarboxylic acid.

Supporting information for this article is available on the WWW under http://dx.doi.org/10.1002/anie.200801488.

tures of **1** and **2** are retained up to 200 and 230 °C, respectively (see the Supporting Information).

The X-ray crystal structures of **1** and **2** are shown in Figure 1 and the Supporting Information.[22] A pair of Zn^{II}

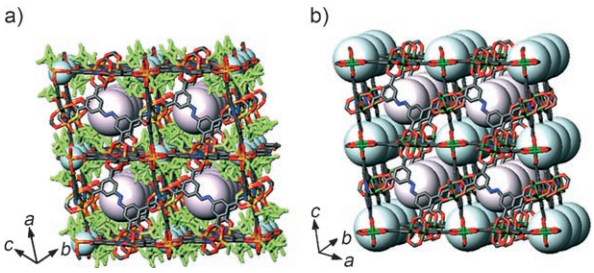

Figure 1. X-ray crystal structures of a) **1** and b) **2** showing their NbO-type 3D frameworks. The two kinds of spheres (in light blue and gray) represent the open spaces that can be occupied by the guest molecules without touching the framework. Hydrogen atoms and guest molecules have been omitted for clarity. The coordinated water molecules in **2** have also been omitted. Color scheme: Zn orange, Cu green, C gray, O red, N blue, coordinated dmf yellowish green.

centers in **1** forms a paddlewheel-shaped $\{Zn_2(O_2CR)_4\}$ cluster, with a Zn···Zn distance of 2.999(1) Å, upon coordination by four carboxylato groups from four independent $abtc^{4-}$ ions. Each Zn^{II} ion is also coordinated to a dmf molecule at the axial site of the paddlewheel cluster. The $Zn-O_{abtc^{4-}}$ bond length averages 2.033(1) Å and the $Zn-O_{dmf}$ bond length averages 1.977(2) Å. The $abtc^{4-}$ ion is coplanar and acts as a rectangular building block. Every square-shaped SBU in the $\{Zn_2(O_2CR)_4\}$ cluster is linked by four rectangular $abtc^{4-}$ ions, which extend infinitely to give rise to an NbO-type 3D network. Large rhombic cavities with an effective diameter of 9.1 Å(estimated by Material Studio software, version 4.1) are formed in the structure, with Zn_2 SBUs as the nodes and organic ligands as the struts of the cube. Smaller cavities with an effective diameter of around 3.0 Å are also formed by paddlewheel SBUs as the coordinated dmf molecules point into the cavities and reduce the space available (see the Supporting Information). Since the coordinated dmf molecules block the channels parallel to the $[10\bar{1}]$ direction, these cavities are only connected in the [102] direction to generate undulating 1D channels, which are occupied by the guest molecules. The void volume of **1** with and without coordinated dmf molecules is 49.1 % and 68.1 %, respectively, as estimated by PLATON.[23]

Thermogravimetric analysis of **1** reveals a 28.5 % weight loss at 25–175 °C, which corresponds to the loss of all (four H_2O and ten dmf) guest molecules (calcd 29.8 %) per formula unit. This step is followed by an additional weight loss of 15.2 % at 175–370 °C, which corresponds to the loss of six coordinated dmf molecules (calcd. 16.3 %).

The X-ray structure of **2**[22] indicates that it is isostructural with **1**. A pair of Cu^{II} centers form a $\{Cu_2(O_2CR)_4\}$ paddlewheel cluster similar to that in **1**, but a water molecule is coordinated to the axial site of each square-pyramidal Cu^{II} ion instead of dmf. The Cu···Cu distance in the paddlewheel cluster averages 2.659(1) Å. The $Cu-O_{abtc^{4-}}$ bond distance averages 1.980(2) Å and is therefore much shorter than the average $Zn-O_{abtc^{4-}}$ bond distance in **1**. The $Cu-O_{water}$ bond distance averages 2.155(3) Å. The framework of **2** contains two kinds of cavities, one of which is formed from Cu_2 SBUs located at the nodes and organic ligands as the struts of the cube, and the other of which is formed from paddlewheel SBUs (see the Supporting Information). The coordinated water molecules point towards the inside of the smaller cavities and do not block the 3D channels. The sizes of the two different cavities are almost the same (10.2 Å as estimated by Material Studio software, version 4.1) after removal of all coordinated water molecules. The void volume of **2** with and without coordinated water molecules is 67.2 % and 71.1 %, respectively, as estimated by PLATON.[23]

Thermogravimetric analysis of **2** reveals a 29.6 % weight loss at 25–200 °C, which corresponds to the loss of two coordinated H_2O molecules, six 1,4-dioxane and four dmf guest molecules (calcd 33.0 %) per formula unit. This step is followed by an additional 15.8 % weight loss at 200–310 °C, which corresponds to the loss of six dmf guest molecules (calcd 15.6 %). This result indicates that once the coordinated water molecules have been removed at lower temperature, the dmf guest molecules move to the vacant coordination sites of Cu^{II} to generate **2a**, from which the dmf molecules can only be removed at higher temperatures.

Compounds **1a**, **2a**, and **2b** were prepared for gas sorption studies as follows. **1a** was prepared by heating **1** at 100 °C under vacuum for 18 h. Further heating of **1a** to remove the coordinated dmf molecules leads to collapse of the framework, as evidenced by the PXRD patterns. The desolvated compounds **2a** and **2b** were prepared by heating **2** at 155 °C under N_2 flow for 3 h and at 170 °C under vacuum for 24 h, respectively. Preparation of the water-containing compound $[\{Cu_2(abtc)(H_2O)_2\}_3]$ was unsuccessful—heat treatment of **2** produced only **2a**, and guest exchange of **2** with MeOH and CH_2Cl_2, followed by evacuation at room temperature, led to collapse of the framework (see the Supporting Information). The PXRD patterns (see Supporting Information) indicate that the framework structure of **1a** is the same as that of **1** and that those of **2a** and **2b** are the same as that of **2**. Care should be taken when handling **2b** because the PXRD pattern indicates that the framework structure of **2b** is destroyed upon exposure to air.

The N_2, CO_2, CH_4, and H_2 gas sorption capabilities of **1a**, **2a**, and **2b** are summarized in Table 1. To eliminate the mass effect of the solid with no coordinated dmf (**2b**) compared to those with dmf (**1a** and **2a**), gas sorption capacities are also provided in terms of mass of adsorbed gas per unit sample volume ($g\,L^{-1}$) in addition to wt %. The IR spectra and elemental analyses indicated that **1a** and **2a** still contain coordinated dmf molecules even after the gas sorption experiments (see the Supporting Information).

Solid **1a**, **2a**, and **2b** adsorb N_2 gas (362 (462), 322 (404), and 669 $cm^3\,g^{-1}$ (642 $g\,L^{-1}$), respectively) at 77 K and 1 atm and show reversible type I isotherms, thus indicating microporosity. The surface area and pore volume, as estimated by applying the Langmuir and Dubinin–Radushkevich equations, are, respectively, 1460 $m^2\,g^{-1}$ (1491 $m^2\,cm^{-3}$) and 0.53 $cm^3\,g^{-1}$ (0.54 $cm^3\,cm^{-3}$) for **1a**, 1260 $m^2\,g^{-1}$

Table 1: Gas-adsorption data for **1a**, **2a**, and **2b**.

Gas	T [K]	wt% gas[a]			Gas adsorbed per unit host volume[b] [g L^{-1}]		
		1a	**2a**	**2b**	**1a**	**2a**	**2b**
N_2	77	45.3	40.3	83.7	463	403	643
H_2	77	2.07	1.83	2.87	21.1	18.3	22.0
		3.70[c]		5.22[c]	37.8[c]		40.1[c]
		4.49[d]		6.76[d]	45.8[d]		51.9[d]
CO_2	195	55.1	53.8	112.3	563	539	862
CO_2	273	20.6	19.2	38.5	210	192	295
CH_4	195	11.4	10.9	21.8	116	109	167
CH_4	273	1.74	1.85	2.56	17.8	18.5	20.0

[a] Amount of gas adsorbed at a pressure of 0.95 atm for N_2 and 1 atm for all other gases. [b] The values are calculated by multiplying the mass of adsorbed gas per gram by the density of the sample (1021 g L^{-1} for **1a**, 1001 g L^{-1} for **2a**, and 768 g L^{-1} for **2b**), assuming that the cell volumes of **1** and **2** are retained in **1a**, **2a**, and **2b**. [c] Excess adsorption capacity at 77 K and 50 bar. [d] Total adsorption capacity at 77 K and 50 bar.[26,27]

(1261 m^2 cm^{-3}) and 0.48 cm^3 g^{-1} (0.48 cm^3 cm^{-3}) for **2a**, and 2850 m^2 g^{-1} (2189 m^2 cm^{-3}) and 1.00 cm^3 g^{-1} (0.77 cm^3 cm^{-3}) for **2b**. The available surface area and pore volume in **2b**, which has AMSs, are 1.4–1.7 times greater than those of **1a** and **2a**, which contain no AMSs. The fact that **2a** has a lower porosity than **1a** must be due to the fact that the Cu–O_{dmf} bond in **2a** is longer than the Zn–O_{dmf} bond in **1a** due to the Jahn–Teller distortion, which reduces the free space in **2a**. The pore-size distributions derived from the N_2 isotherms at 77 K by the Saito–Foley (SF) method[24] suggest that the pore sizes for **1a**, **2a**, and **2b** are 12.8, 10.5, and 12.9 Å, respectively (see the Supporting Information). Although the X-ray structure of **1a** indicates that it contains two different sizes of cavities (9.1 and 3.0 Å), presence of the smaller cavity cannot be demonstrated from the N_2 sorption data because the N_2 molecule has a kinetic diameter (3.64 Å) greater than the cavity size.

Solid **1a**, **2a**, and **2b** also have high CO_2 and CH_4 sorption capacities at 1 atm of gas pressure and at 195 and 273 K (Table 1 and Figure 2). The adsorption data are superior to those for other MOFs measured under similar conditions. At 273 K and 1 atm, **2b** adsorbs 295 g of CO_2 per liter of sample,

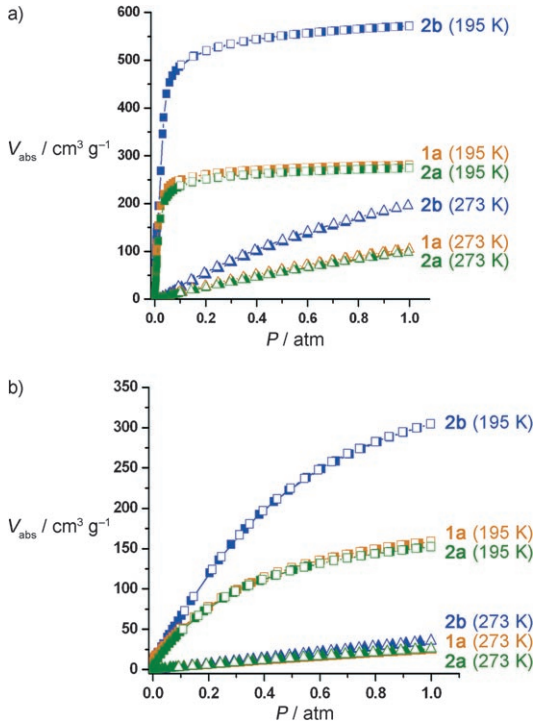

Figure 2. a) CO_2 and b) CH_4 adsorption isotherms for **1a** (orange), **2a** (green), and **2b** (blue) at 195 (■) and 273 K (▲). Filled shape: adsorption; open shape: desorption.

which is equivalent to 150.2 L L^{-1}. This value is almost twice as high as the highest CO_2 uptake reported to date (83 L L^{-1} for ZIF-69).[25] The CO_2 and CH_4 adsorption capacities of **2b** are higher than those of **1a** and **2a** (140–160% per unit sample volume), as is the case for N_2 adsorption. That sorption capacity of **2b** for N_2, CO_2, and CH_4 is greater than that of **1a** and **2a** is probably because N_2, CO_2, and CH_4 molecules, whose kinetic diameters are 3.64, 3.3, and 3.8 Å, respectively, are accessible to all channels in **2b** (pore size: 10.2 Å), whilst they cannot enter the smaller channels (aperture size: 3.0 Å) in **1a** and **2a**.

Solid **1a**, **2a**, and **2b** show high H_2 sorption capacities of 2.07, 1.83, and 2.87 wt%, respectively, at 77 K and 1 atm (Figure 3). The H_2 sorption isotherms show no hysteresis on

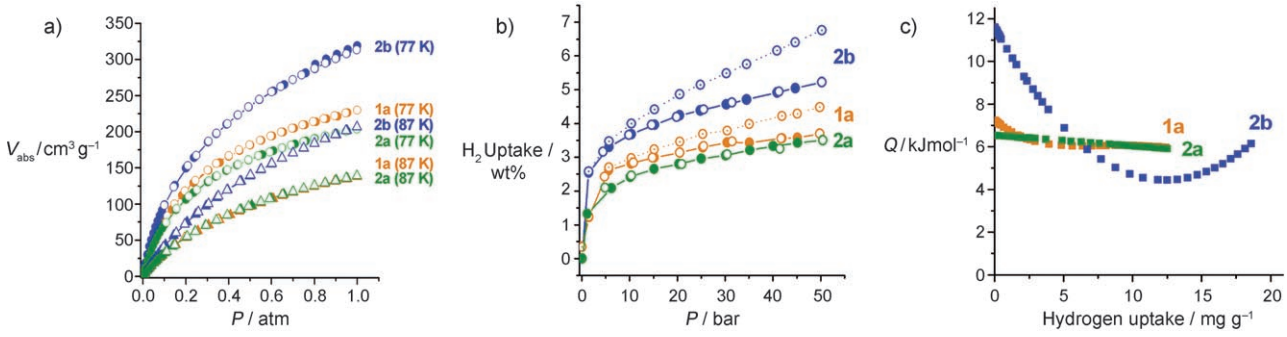

Figure 3. a) H_2 gas sorption isotherms measured at 77 (●) and 87 K (▲) up to 1 atm of H_2 for **1a** (orange), **2a** (green), and **2b** (blue). b) Excess (——) and total (••••) H_2 adsorption isotherms at 77 K and high pressure.[26] Filled shape: adsorption; open shape: desorption. c) Isosteric heat of H_2 adsorption for **1a** (orange), **2a** (green), and **2b** (blue).

adsorption and desorption. To the best of our knowledge, the H_2 adsorption capacity (2.87 wt%) of **2b** at 77 K and 1 atm is the highest of any MOF measured under the same conditions.[1–3,13,14] When the H_2 pressure is increased to 50 bar at 77 K, the excess adsorption capacities of **1a** and **2b** become 3.70 and 5.22 wt%, respectively (Figure 3b), which gives maximum capacities of 4.30 and 6.37 wt%, respectively, on fitting the data to the Langmuir equation. The total adsorption capacities of **1a** and **2b** at 77 K and 50 bar are 4.49 (45.8) and 6.76 wt% (51.9 $g L^{-1}$), respectively.[26,27] The H_2 adsorption capacity of **2b** (in wt%) is distinctly higher than that of **1a** or **2a**, although this is mainly due to the lower molecular weight effect as the sorption capacity ratios **2b**:**1a** and **2b**:**2a** per unit sample volume (Table 1) are only 105% and 120%, respectively, at 77 K and 1 atm.

The H_2 sorption behavior was also measured at 87 K and the isosteric heats of adsorption were estimated according to the virial equation[28] to verify the effect of the AMSs. The isosteric heats (Figure 3c) are 5.96–7.24 kJ mol^{-1} for **1a**, 5.91–6.53 kJ mol^{-1} for **2a**, and 4.43–11.60 kJ mol^{-1} for **2b**, depending on the degree of H_2 loading. The zero-coverage isosteric heat of H_2 adsorption for **2b** (11.60 kJ mol^{-1}) is greater than those for **1a** (7.24 kJ mol^{-1}) and **2a** (6.53 kJ mol^{-1}), and the highest yet observed for the MOFs, thus clearly suggesting that the interaction between the host and H_2 molecules is stronger for the MOF containing AMSs than those without AMSs.

In conclusion, we have demonstrated the gas sorption properties of isostructural NbO-type MOFs with AMSs ($[\{Cu_2(abtc)\}_3]$ (**2b**)) and without AMSs ($[\{Zn_2(abtc)(dmf)_2\}_3]$ (**1a**), $[\{Cu_2(abtc)(dmf)_2\}_3]$ (**2a**)). All these compounds show much higher H_2 and CO_2 uptake capacities than other MOFs. The MOF with AMSs (**2b**) clearly has a higher H_2 adsorption in terms of wt% as well as per unit sample volume ($g L^{-1}$) compared to those with no AMSs (**1a** and **2a**). This is likely to be due to a stronger interaction with H_2 molecules in the former, although its lower molecular weight is the major contributor to the higher wt% of adsorbed H_2.

Received: March 29, 2008
Revised: May 9, 2008
Published online: September 2, 2008

Please note: Minor changes have been made to this manuscript since its publication in *Angewandte Chemie* Early View. The Editior.

Keywords: adsorption · carboxylate ligands · hydrogen · metal–organic frameworks · microporous materials

[1] E. Y. Lee, S. Y. Jang, M. P. Suh, *J. Am. Chem. Soc.* **2005**, *127*, 6374 – 6381.

[2] a) E. Y. Lee, M. P. Suh, *Angew. Chem.* **2004**, *116*, 2858 – 2861; *Angew. Chem. Int. Ed.* **2004**, *43*, 2798 – 2801; b) A. G. Wong-Foy, A. J. Matzger, O. M. Yaghi, *J. Am. Chem. Soc.* **2006**, *128*, 3494 – 3495; c) R. Matsuda, R. Kitaura, S. Kitagawa, Y. Kubota, R. V. Belosludov, T. C. Kobayashi, H. Sakamoto, T. Chiba, M. Takata, Y. Kawazoe, Y. Mita, *Nature* **2005**, *436*, 238 – 241.

[3] a) M. Dincă, A. Dailly, Y. Liu, C. M. Brown, D. A. Neumann, J. R. Long, *J. Am. Chem. Soc.* **2006**, *128*, 16876 – 16883; b) M. Dincă, J. R. Long, *J. Am. Chem. Soc.* **2007**, *129*, 11172 – 11176.

[4] M. P. Suh, Y. E. Cheon, E. Y. Lee, *Chem. Eur. J.* **2007**, *13*, 4208 – 4215.

[5] a) L. Pan, B. Paeker, X. Huang, D. H. Olson, J. Lee, J. Li, *J. Am. Chem. Soc.* **2006**, *128*, 4180 – 4181; b) J. C. Rowsell, O. M. Yaghi, *J. Am. Chem. Soc.* **2006**, *128*, 1304 – 1315.

[6] a) Y. E. Cheon, M. P. Suh, *Chem. Eur. J.* **2008**, *14*, 3961 – 3967; b) H. R. Moon, N. Kobayashi, M. P. Suh, *Inorg. Chem.* **2006**, *45*, 8672 – 8676.

[7] a) H. J. Choi, M. P. Suh, *J. Am. Chem. Soc.* **2004**, *126*, 15844 – 15851; b) K. S. Min, M. P. Suh, *Chem. Eur. J.* **2001**, *7*, 303 – 313; c) H. Kim, M. P. Suh, *Inorg. Chem.* **2005**, *44*, 810 – 812; d) M. P. Suh, J. W. Ko, H. J. Choi, *J. Am. Chem. Soc.* **2002**, *124*, 10976 – 10977; e) H. J. Choi, T. S. Lee, M. P. Suh, *Angew. Chem.* **1999**, *111*, 1490 – 1493; *Angew. Chem. Int. Ed.* **1999**, *38*, 1405 – 1408; f) J. W. Ko, K. S. Min, M. P. Suh, *Inorg. Chem.* **2002**, *41*, 2151 – 2157; g) B. Chen, C. Liang, J. Yang, D. S. Contreras, Y. L. Clancy, E. B. Lobkovsky, O. M. Yaghi, S. Dai, *Angew. Chem.* **2006**, *118*, 1418 – 1421; *Angew. Chem. Int. Ed.* **2006**, *45*, 1390 – 1393; h) J. Y. Lee, D. H. Olson, L. Pan, T. J. Ernge, J. Li, *Adv. Funct. Mater.* **2007**, *17*, 1255 – 1262.

[8] a) K. S. Min, M. P. Suh, *J. Am. Chem. Soc.* **2000**, *122*, 6834 – 6840; b) H. J. Choi, M. P. Suh, *Inorg. Chem.* **2003**, *42*, 1151 – 1157; c) Y. Liu, G. Li, X. Li, Y. Cui, *Angew. Chem.* **2007**, *119*, 6417 – 6420; *Angew. Chem. Int. Ed.* **2007**, *46*, 6301 – 6304.

[9] a) C. D. Wu, A. Hu, L. Zhang, W. Lin, *J. Am. Chem. Soc.* **2005**, *127*, 8940 – 8941; b) T. Uemura, R. Kitaura, Y. Ohta, M. Nagaoka, S. Kitagawa, *Angew. Chem.* **2006**, *118*, 4218 – 4222; *Angew. Chem. Int. Ed.* **2006**, *45*, 4112 – 4116; c) S. Kitagawa, S. Noro, T. Nakamura, *Chem. Commun.* **2006**, 701 – 707; d) D. N. Dybtsev, A. L. Nuzhdin, H. Chun, K. P. Bryliakov, E. P. Talsi, V. P. Fedin, K. Kim, *Angew. Chem.* **2006**, *118*, 930 – 934; *Angew. Chem. Int. Ed.* **2006**, *45*, 916 – 920.

[10] a) C. A. Bauer, T. V. Timofeeva, T. B. Settersten, B. D. Patterson, V. H. Liu, B. A. Simmons, M. D. Allendorf, *J. Am. Chem. Soc.* **2007**, *129*, 7136 – 7144; b) B. Chen, Y. Yang, F. Zapata, G. Lin, G. Qian, E. B. Lobkovsky, *Adv. Mater.* **2007**, *19*, 1693 – 1696.

[11] a) M. P. Suh, H. R. Moon, E. Y. Lee, S. Y. Jang, *J. Am. Chem. Soc.* **2006**, *128*, 4710 – 4718; b) H. R. Moon, J. H. Kim, M. P. Suh, *Angew. Chem.* **2005**, *117*, 1287 – 1291; *Angew. Chem. Int. Ed.* **2005**, *44*, 1261 – 1265.

[12] a) O. M. Yaghi, M. O'Keeffe, N. W. Ockwig, H. K. Chae, M. Eddaoudi, J. Kim, *Nature* **2003**, *423*, 705 – 714; b) H. R. Moon, M. P. Suh, *Adv. Inorg. Chem.* **2007**, *59*, 39 – 59.

[13] B. Chen, N. W. Ockwig, A. R. Millward, D. S. Contreras, O. M. Yaghi, *Angew. Chem.* **2005**, *117*, 4823 – 4827; *Angew. Chem. Int. Ed.* **2005**, *44*, 4745 – 4749.

[14] X. Lin, J. Jia, X. Zhao, K. M. Thomas, A. J. Blake, G. S. Walker, N. R. Champness, P. Hubberstey, M. Schröder, *Angew. Chem.* **2006**, *118*, 7518 – 7524; *Angew. Chem. Int. Ed.* **2006**, *45*, 7358 – 7364.

[15] S. S. Y. Chui, S. M. F. Lo, J. P. H. Charmant, A. G. Orpen, I. D. Williams, *Science* **1999**, *283*, 1148 – 1150.

[16] B. Chen, N. W. Ockwig, F. R. Fronczek, D. S. Contreras, O. M. Yaghi, *Inorg. Chem.* **2005**, *44*, 181 – 183.

[17] H. Chun, D. N. Dybtsev, H. Kim, K. Kim, *Chem. Eur. J.* **2005**, *11*, 3521 – 3529.

[18] Y. Liu, J. F. Eubank, A. J. Cairns, J. Eckert, V. C. Kravtsov, R. Luebke, M. Eddaoudi, *Angew. Chem.* **2007**, *119*, 3342 – 3347; *Angew. Chem. Int. Ed.* **2007**, *46*, 3278 – 3283.

[19] C.-L. Chen, A. M. Goforth, M. D. Smith, C.-Y. Su, H.-C. zur Loye, *Angew. Chem.* **2005**, *117*, 6831 – 6835; *Angew. Chem. Int. Ed.* **2005**, *44*, 6673 – 6677.

[20] S. Wang, X. Wang, L. Li, R. C. Advincula, *J. Org. Chem.* **2004**, *69*, 9073 – 9084.

[21] Some of these results were reported at the 100th annual meeting of the Korean Chemical Society, October 19, **2007**, Abstract p. 247.

[22] Crystal data for **1**: $C_{66}H_{60}N_{12}O_{30}Zn_6$, $M_r = 1893.60$, monoclinic, space group $C2/c$ (no. 15), $a = 33.540(7)$, $b = 19.607(4)$, $c = 21.705(4)$ Å, $\beta = 120.30(3)°$, $V = 12324(4)$ Å^3, $Z = 4$, $d_{calcd} = 1.021$ g cm^{-3} for the framework and coordinated dmf molecules only, $T = 100(2)$ K, crystal size $0.2 \times 0.2 \times 0.1$ mm^3, $\lambda = 0.69998$ Å, $2\theta = 60.64°$, 536 parameters, $R_1 = 0.0624$ ($I > 2\sigma(I)$, 17732 reflections), $wR_2 = 0.1857$ (all data, 34417 reflections), GOF = 0.987. **2**: $C_{48}H_{30}Cu_6N_6O_{30}$, $M_r = 1552.08$, monoclinic, space group $I2/m$ (no. 12), $a = 23.1092(6)$, $b = 18.8031(5)$, $c = 29.8062(6)$ Å, $\beta = 105.325(2)°$, $V = 12491.0(5)$ Å^3, $Z = 4$, $d_{calcd} = 0.825$ g cm^{-3} for the framework and coordinated H_2O molecules only, $T = 293(2)$ K, crystal size $0.2 \times 0.2 \times 0.1$ mm^3, $\lambda = 0.71073$ Å, $2\theta = 54.00°$, 417 parameters, $R_1 = 0.1181$ ($I > 2\sigma(I)$, 13996 reflections), $wR_2 = 0.3357$ (all data, 24518 reflections), GOF = 0.893. Crystallographic data for **1** and **2** are summarized in the Supporting Information. CCDC-679644 (**1**) and -679643 (**2**) contain the supplementary crystallographic data for this paper. These data can be obtained free of charge from The Cambridge Crystallographic Data Centre via www.ccdc.cam.ac.uk/data_request/cif.

[23] A. L. Spek, *PLATON 99, A Multipurpose Crystallographic Tool*, Utrecht University, The Netherlands, **1999**.

[24] A. Saito, H. C. Foley, *AIChE J.* **1991**, *37*, 429 – 436.

[25] a) R. Banerjee, A. Phan, B. Wang, C. Knobler, H. Furukawa, M. O'Keeffe, O. M. Yaghi, *Science* **2008**, *319*, 939 – 943; b) B. Wang, A. P. Côté, H. Furukawa, M. O'Keeffe, O. M. Yaghi, *Nature* **2008**, *453*, 207 – 212.

[26] Excess adsorption is the amount of physisorbed gas on the surface, which is the quantity being measured. Total adsorption is the sum of the amount of adsorbed gas on the surface and the pressurized gas within the pores (see ref. [27] and the Supporting Information).

[27] a) H. Furukawa, M. A. Miller, O. M. Yaghi, *J. Mater. Chem.* **2007**, *17*, 3197 – 3204; b) S. S. Kaye, A. Dailly, O. M. Yaghi, J. R. Long, *J. Am. Chem. Soc.* **2007**, *129*, 14176 – 14177.

[28] L. Czepirski, J. Jagiello, *Chem. Eng. Sci.* **1989**, *44*, 797 – 801.

